Acta Crystallographica Section D
Biological Crystallography
ISSN 0907-4449

Structural studies of *Proteus mirabilis* catalase in its ground state, oxidized state and in complex with formic acid

Pierre Andreoletti,[a] Anaïs Pernoud,[b] Germaine Sainz,[c] Patrice Gouet[b] and Hélène Marie Jouve[d]*

[a]Avidis S.A., Biopôle Clermont-Limagne, 63360 Saint-Beauzire, France, [b]IBCP–Laboratoire de Bio-Cristallographie, 7 Passage du Vercors, 69367 Lyon CEDEX 07, France, [c]European Synchrotron Radiation Facility, 6 Rue Jules Horowitz, BP 220, F-38043 Grenoble CEDEX, France, and [d]Institut de Biologie Structurale Jean-Pierre Ebel, CEA/CNRS/UJF, 41 Rue Jules Horowitz, 38027 Grenoble CEDEX 1, France

Correspondence e-mail: jouve@ibs.fr

Received 20 March 2003
Accepted 5 September 2003

PDB References: frozen native PMC, 1m85; PMC–formic acid complex, 1klw; PMC compound I, 1mqf.

The structure of *Proteus mirabilis* catalase in complex with an inhibitor, formic acid, has been solved at 2.3 Å resolution. Formic acid is a key ligand of catalase because of its ability to react with the ferric enzyme, giving a high-spin iron complex. Alternatively, it can react with two transient oxidized intermediates of the enzymatic mechanism, compounds I and II. In this work, the structures of native *P. mirabilis* catalase (PMC) and compound I have also been determined at high resolution (2.0 and 2.5 Å, respectively) from frozen crystals. Comparisons between these three PMC structures show that a water molecule present at a distance of 3.5 Å from the haem iron in the resting state is absent in the formic acid complex, but reappears in compound I. In addition, movements of solvent molecules are observed during formation of compound I in a cavity located away from the active site, in which a glycerol molecule is replaced by a sulfate. These results give structural insights into the movement of solvent molecules, which may be important in the enzymatic reaction.

1. Introduction

Haem catalases and peroxidases are enzymes of functional importance because they serve in part to protect the cell against the deleterious effects of peroxides produced by the partial reduction of molecular oxygen in aerobic organisms. Both types of enzymes are classed in the same enzyme superfamily (Dunford, 1999), but they differ in sequence and exhibit different folds: $\alpha+\beta$ for haem catalases (Bravo *et al.*, 1997) and primarily all-α for haem-dependant peroxidases (Poulos, 2000). The first step in the catalytic mechanism is the same for both enzymes: a transient two-electron oxidized intermediate named compound I is formed (1). Compound I contains an oxoferryl group ($Fe^{IV}{=}O$) associated with a porphyrin π-cation radical (1) (Hewson & Hager, 1979; Schonbaum & Chance, 1976; Nicholls *et al.*, 2001),

$$E-Fe^{III} + H_2O_2 \rightarrow E[\pi^{+\cdot}]-Fe^{IV}{=}O + H_2O, \qquad (1)$$

where $E-Fe^{III}$ is the native state and $E[\pi^{+\cdot}]-Fe^{IV}{=}O$ is compound I.

Thus, catalases as well as peroxidases can reduce hydrogen peroxide (H_2O_2) to water during this step. However, only catalases can return to the resting state *via* a two-electron transfer mechanism by using a second molecule of H_2O_2 (2) (the so-called catalatic way) to achieve the disproportionation of H_2O_2 into molecular dioxygen and water (Nicholls & Schonbaum, 1963),

$$E[\pi^{+\cdot}]-Fe^{IV}{=}O + H_2O_2 \rightarrow E-Fe^{III} + H_2O + O_2. \quad (2)$$

In contrast, peroxidases require a two-step single-electron transfer mechanism to return to the native state *via* the oxidation of another electron donor (AH) instead of H_2O_2 (equations 3 and 4) (the peroxidatic way). The peroxidatic way involves the transient formation of compound II, $E-Fe^{IV}{=}O$, obtained by a single reduction of compound I. Compound II retains the oxoferryl group but loses the porphyrin radical (Dunford, 1999),

$$E[\pi^{+\cdot}]-Fe^{IV}{=}O + AH \rightarrow E-Fe^{IV}{=}O + A^{\cdot} + H^{+} \quad (3)$$

$$E-Fe^{IV}{=}O + AH + H^{+} \rightarrow E-Fe^{III} + A^{\cdot} + H_2O. \quad (4)$$

Catalases are able to use the peroxidatic way under certain conditions, such as with a slow flow of hydrogen peroxide (the case *in vivo*) or with different one-electron donors (Nicholls *et al.*, 2001). However, the pathway *via* compound II leads to decreasing catalatic activity (Nicholls & Schonbaum, 1963). Certain catalases can avoid inactivation to compound II by using tightly bound NADPH to reduce compound I to native enzyme (Andreoletti *et al.*, 2001). According to a recent theory, the catalatic way requires the release of a water molecule produced during formation of compound I (Jones, 2001), while the peroxidatic way requires the presence of this water molecule associated with compound I.

Of the chemicals that react with catalase, formate (in its protonated form, formic acid; Maj *et al.*, 1998) is a physiological ligand of the enzyme (Williams-Smith & Morrison, 1975). It inhibits the reaction of catalase with hydroperoxides (Nicholls & Schonbaum, 1963; Jouve *et al.*, 1984). It reacts with three functional forms of catalase: ferric enzyme, compound I and compound II (Nicholls *et al.*, 2001). The rate constants for its reaction with the ferric enzyme and compound I are essentially identical (Schonbaum & Chance, 1976) and its apparent affinities for ferric enzyme and compound II are similar (Nicholls, 1961; Maj *et al.*, 1998). It is not clear whether formate is directly bound to the haem iron or is bound *via* a water molecule (Hershberg & Chance, 1975; Vuk-Pavlovic & Williams-Smith, 1977). Until now, no structure has been determined of formate in complex with catalase or with other haemoproteins able to bind formate.

Proteus mirabilis catalase (PMC), an NADPH-binding catalase that structurally resembles mammalian catalases, is a particularly efficient haem catalase (Switala & Loewen, 2002). It forms a very stable compound I and this property has previously allowed determination of the PMC compound I structure by time-resolved studies (Gouet *et al.*, 1996; Jouve *et al.*, 1997). The crystallographic structure of PMC in complex with formic acid is reported here from data collected from frozen crystals. To improve the comparison between the known PMC structures, especially at the level of their active site, the native PMC and PMC compound I structures previously determined at room temperature have also been determined at low temperature from frozen crystals. The obtained resolutions of the native and compound I PMC structures (2.0 and 2.5 Å, respectively) were higher than previously reported (2.2 and 2.8 Å, respectively; Gouet *et al.*, 1995, 1996) and allowed the identification of new water molecules. The results provide structural insights into water-molecule movements within the catalase distal site during catalysis.

2. Materials and methods

2.1. Chemicals

Sodium formate and common salts were obtained from Sigma–Aldrich and hydrogen peroxide (30% Suprapur Perhydrol) from Merck. PMC was purified from *P. mirabilis* PR bacteria as described previously (Jouve *et al.*, 1989) with the improvements proposed by Andreoletti *et al.* (2003). Only the PMC form without NADPH was retained for the study. The purified fractions of catalase had a Reinheitszahl index (A_{406}/A_{280}) greater than 1.0. The catalase was homogenous as observed by SDS–PAGE. The enzyme solutions (about 50 mg ml^{-1}) were stored at 253 K with 8%(*v*/*v*) glycerol in 0.1 *M* Tris–HCl buffer pH 7.5.

2.2. Crystallization, data collection and structure determination

Crystals of native PMC were grown by vapour diffusion from well solutions using ammonium sulfate as precipitating agent and 0.1 *M* Tris–maleate buffer pH 6.5 (Jouve *et al.*, 1991). PMC crystals were flash-frozen in liquid nitrogen as previously described by Andreoletti *et al.* (2003). Compound I was obtained by soaking a crystal for 5 min in a well solution containing 3.7 *M* ammonium sulfate, 1.6 m*M* peroxoacetic acid, 0.1 *M* Tris–maleate pH 5.9. The crystal turned from brown to green within 5 min and was flash-frozen. Complete transformation into compound I was confirmed by recording the absorbance spectrum of the frozen crystal with a microspectrophotometer (Gouet *et al.*, 1996). The formate complex was obtained by soaking PMC crystals in a solution containing 200 m*M* sodium formate, 3.7 *M* ammonium sulfate in 0.1 *M* Tris–maleate buffer pH 6.5 and was flash-frozen in liquid nitrogen. The binding of formate to catalase increased when the pH was lowered, showing a preference for the acid form (Hershberg & Chance, 1975; Nicholls, 1961). A slightly acidic solution (pH 6.5) was chosen for soaking the PMC crystals, as the enzyme precipitates at lower pH (below pH 5). A change in crystal colour (from brown to green) was considered to be indicative of ligand binding. The unit-cell dimensions of frozen crystals are smaller than those of capillary-mounted crystals: $a = b = 110$, $c = 250$ Å, compared with $a = b = 112$, $c = 250$ Å. The space group is $P6_222$, with one monomer per asymmetric unit.

Synchrotron data were collected at beamline BM14 at ESRF, Grenoble. Data processing was performed with the *HKL* suite (Otwinowski & Minor, 1997). Structures of frozen native PMC, the formic acid complex and compound I were determined by molecular replacement with a rigid-body method, using the structure of native PMC determined at room temperature (Gouet *et al.*, 1995) as a starting model.

Crystallographic refinements and map calculations were performed with *CNS* (Brünger *et al.*, 1998). $2F_o - F_c$ and $F_o - F_c$ maps were visualized on graphics stations using the program *TURBO-FRODO* (Roussel & Cambillau, 1989). The flexible loop comprising residues 359–362 was poorly defined in the room-temperature structures and was rebuilt with *TURBO-FRODO*. With the exception of this segment, the C^{α} traces of all PMC structures were equivalent [r.m.s. displacements of 0.2–0.3 Å on all C^{α} pairs after superimposition with *LSQKAB* (Collaborative Computational Project, Number 4, 1994)]. A model of formic acid was generated with the program *PRODRG* (van Aalten *et al.*, 1996) and positioned in the electron-density maps of the PMC–formic acid complex. The 2 Å electron-density map of frozen native PMC allowed the identification of a glycerol molecule and of more than 400 new water molecules. Final statistics for the three frozen structures are shown in Table 1.

Table 1
Statistics of data processing and crystallographic refinement.

Values in parentheses are for the highest resolution shell.

	Native PMC	PMC–formic acid complex	PMC compound I
Data processing			
Resolution range (Å)	30.0–2.0	30.0–2.3	30.0–2.5
Total no. of reflections	247359	294452	138931
No. of unique reflections	60596	39651	30822
Completeness (%)	99.7 (98.4)	98.4 (98.2)	98.3 (97.0)
Redundancy	4.1 (4.1)	7.5 (7.4)	4.5 (4.1)
$I/\sigma(I)$	9.7 (3.0)	6.9 (3.5)	10.7 (6.7)
$R_{\rm sym}$ (%)	6.0 (30.2)	8.5 (22.2)	4.4 (10.4)
Structure refinement			
Resolution range (Å)	15–2.0	15–2.3	15–2.5
$R_{\rm cryst}$† (%)	19.4	18.1	19.6
$R_{\rm free}$‡ (%)	21.8	21.1	23.4
R.m.s.d. bonds (Å)	0.013	0.008	0.013
R.m.s.d. angles (°)	2.2	1.4	3.3
Mean *B* factor (Å^2)	23.7	21.9	31
E.s.d. from *SIGMAA* (Å)	0.20	0.18	0.25
No. water molecules	531	471	388
No. sulfate ions	8	6	8
No. glycerol molecules	1	1	0
No. formic acid molecules	0	1	0

† $R_{\rm cryst} = \sum_{hkl} ||F_{\rm obs}| - |F_{\rm calc}|| / \sum_{hkl} |F_{\rm obs}|$, where $F_{\rm obs}$ represents the observed structure-factor amplitudes and $F_{\rm calc}$ the calculated structure-factor amplitudes. ‡ $R_{\rm free}$ is the same as $R_{\rm cryst}$, but calculated for a test set comprising reflections not used in the refinement (5%).

3. Results and discussion

3.1. Structure of native PMC at 2.0 Å resolution

The crystal structure of native PMC presented here was obtained from frozen crystals at 2.0 Å resolution, a higher resolution than previously reported for crystals mounted in capillaries (2.2 Å resolution; Gouet *et al.*, 1995) and with better data quality for the high-resolution shell (Table 1). Recently, the structure of a recombinant form of native PMC was also published at 2.0 Å resolution (PDB code 1e93; Andreoletti *et al.*, 2003). However, this recombinant enzyme contained about 60% protoporphyrin IX instead of the haem group and the absence of iron influenced the structure. For example, a methionine (Met53) oxidized to sulfone that was clearly observed near the active site in the wild-type structure (Gouet *et al.*, 1995) was partly absent in the recombinant enzyme. The structure of native wild-type PMC presented here shows a methionine sulfone at position 53 with full occupancy.

Another characteristic of the 'frozen' structure is the presence of a single water molecule, modelled at the distal side of the haem with a temperature factor of 34 Å^2, instead of two observed in the previous 'room-temperature' structure (Gouet *et al.*, 1995). The missing water molecule was poorly defined in the electron density of the room-temperature structure and refined with a high temperature factor of 50 Å^2. The resting water molecule is fixed *via* a 2.8 Å hydrogen bond to the $N^{\varepsilon 2}$ atom of the fundamental residue His54 and *via* a 3.5 Å interaction with the haem iron (Fig. 1*a*). It is not hydrogen bonded to the essential Asn127 (4.7 Å to $N^{\delta 2}$; Fig. 2). A single water molecule is also observed in the active site of human erythrocyte catalase (HEC) in a structure at 1.5 Å resolution (PDB code 1dgf; Putnam *et al.*, 2000), whereas two water molecules were observed in other known structures of catalases such as the catalases from *Escherichia coli* (HPII) and *Micrococcus lysodeikticus* (Bravo *et al.*, 1999; Murshudov *et al.*, 1992) determined at 1.9 and 2.0 Å resolution, respectively, a resolution similar to that of the native PMC structure.

A molecule of glycerol is observed in a cavity located about 15 Å below the haem in a postulated 'anion'-binding site (Gouet *et al.*, 1996). The glycerol is in contact with the side chains of Arg342, His349 and His42 of a related monomer (see Fig. 3 for identification of the regions). Glycerol was used during purification of the enzyme (see §2) and its presence deep inside the tetramer of PMC highlights the possibility of exchange between the protein and the solvent. An acetate was modelled at this site in the structure of recombinant PMC (Andreoletti *et al.*, 2003). Therefore, the so-called 'anion'-binding site will from now on be referred to as a 'solute'-binding site.

3.2. Structure of PMC–formic acid complex at 2.3 Å

Formate is a high-spin ligand of PMC as for other catalases (Maj *et al.*, 1998). It forms a green complex with a visible spectrum characterized by a red shift of the Soret band and a blue shift of the α-band. However, the affinity of PMC for formate, with a K_d of 60 m*M* at pH 7.5 (Jouve *et al.*, 1984), was about twofold lower than that of bovine liver catalase at the same pH (Millar *et al.*, 1981). It is known that the affinity of catalase for formate is dependent on pH and increases when the pH is lowered, showing a preference for the protonated form of the ligand (Hershberg & Chance, 1975; Nicholls, 1961). The pK_a of formic acid being 3.7 (at 298 K), it must be kept in mind that at pH 6.5, the pH chosen to soak the PMC crystals, formic acid is almost fully dissociated and formic acid binding involves uptake of both an anion and a proton in the active site (Millar *et al.*, 1981).

The formic acid binding (Fig. 3) did not produce large-scale rearrangements of the protein, so that the C^{α} traces of the frozen native and the formic acid complex can be superimposed with an r.m.s. displacement of 0.2 Å. Millar *et al.* (1981) mentioned a possible secondary binding site for formate anions involving interactions away from the haem and thus invisible by spectroscopic methods. However, no density could be assigned with certainty to a second formic acid (or formate) molecule bound to PMC in the 2.3 Å map at this pH.

The formic acid molecule is well defined with a temperature factor of 18 $Å^2$ and replaces the conserved water molecule of the haem distal side (Figs. 1*a*, 1*b*, 2 and 3). It is hydrogen bonded to His54 *via* an O atom and is in contact with the haem iron *via* another O atom (Fig. 1*b*). Moreover, it is also not far from the strictly conserved Asn127 (3.1 Å from $N^{\delta 2}$; Fig. 2). In common with other high-spin ligands, formate apparently has a similar affinity for native ferric catalase and for compound I. It can reduce compound I using two electrons to give the ferric enzyme, H_2O and CO_2. Formate also catalyses the reduction of compound II to ferric enzyme by 'endogenous' donors in the enzyme (Maj *et al.*, 1998; Nicholls, 1961; Nicholls *et al.*, 2001). However, the absence of peroxide or other substrates that can form compound I or II prevents all further reactions in our experiment.

Other structures of catalase complexes have already been determined. The complex of cyanide with HEC revealed that the iron centre became hexacoordinate with a bound cyanide (Putnam *et al.*, 2000). The water molecule that is initially hydrogen-bonded to the essential distal histidine and asparagine remained unchanged. This could be owing to the fact that cyanide, a low-spin iron ligand, is a smaller molecule and a stronger ligand than formic acid. The HEC structure was also solved in complex with 3-amino-1,2,4-triazole, but in this case the bulky inhibitor drove out the water molecule from its primary position in the active site (Putnam *et al.*, 2000). Finally, binding of H_2O_2 in the structure of an inactive mutant

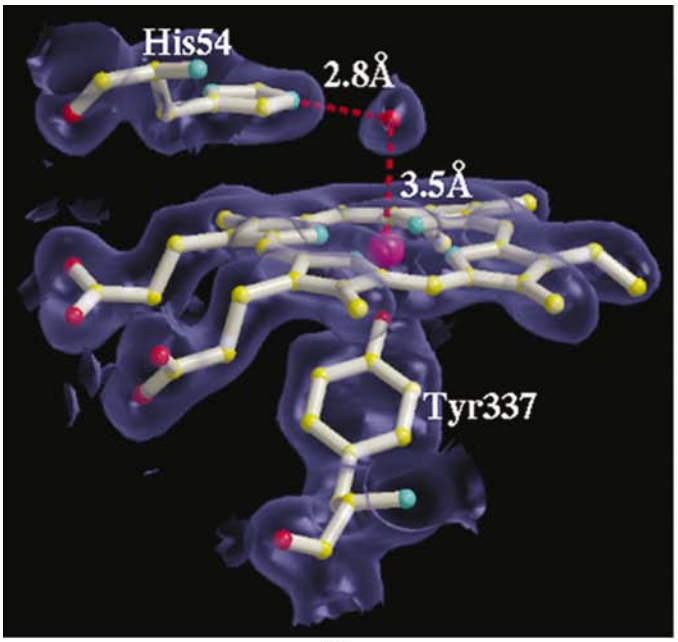

(*a*)

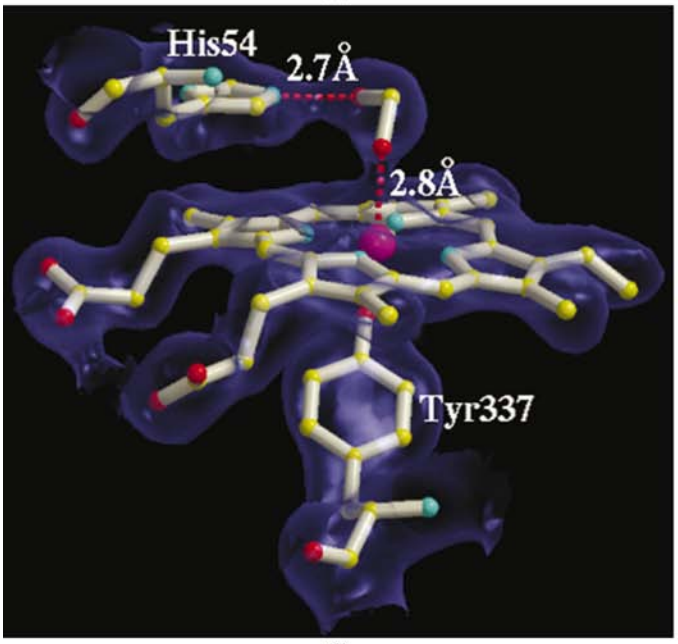

(*b*)

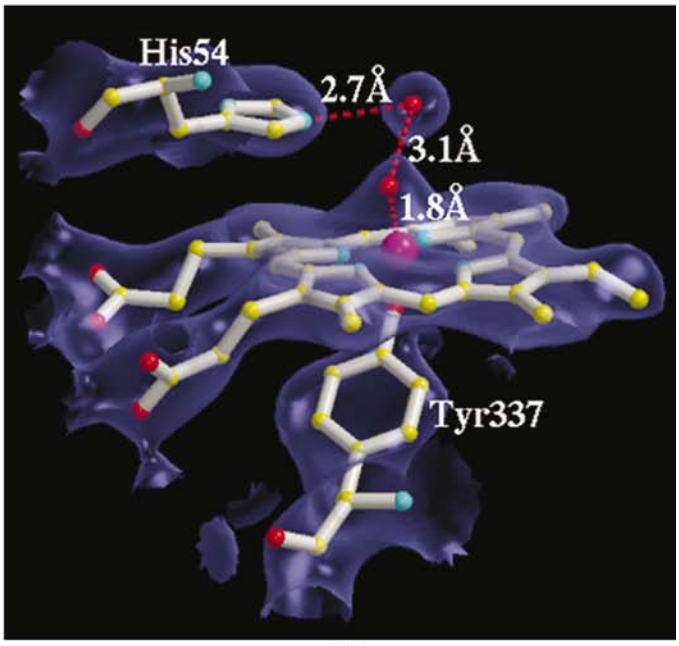

(*c*)

Figure 1
Comparison of the active site of PMC in three different states using the $2F_o - F_c$ electron-density map. Haem and the fundamental residues His54 and Tyr337 are shown in ball-and-stick representation, with N atoms in cyan, O atoms in red, C atoms in yellow and the Fe atom in magenta. The electron-density map is coloured blue and is contoured at 1σ. (*a*) Native PMC at 2 Å resolution. The distances between the O atom of the water molecule and $N^{\varepsilon 2}$ of His54 and the Fe atom are 2.8 and 3.5 Å, respectively. (*b*) Formic acid complex at 2.3 Å resolution. The distances between the formic acid molecule and His54 $N^{\varepsilon 2}$ and the Fe atom are 2.7 and 2.8 Å, respectively. (*c*) Compound I at 2.5 Å resolution. The distances from the O atom of the water molecule to His54 $N^{\varepsilon 2}$ and to the oxoferryl group are 2.7 and 3.1 Å, respectively. This figure was drawn with *BobScript* (Esnouf, 1997).

of HPII displaced six water molecules (Melik-Adamyan *et al.*, 2001).

3.3. Crystallographic structure of PMC compound I at 2.5 Å

Observations made on the active site of the 2.5 Å 'frozen' structure of PMC compound I confirmed those made on the previous 2.7 Å time-resolved structure (Gouet *et al.*, 1996): the oxoferryl group is clearly visible in the electron-density maps, as well as a water molecule between this oxoferryl group and His54 (Fig. 1*c*). This water molecule is located at a similar position to the conserved water molecule of native PMC, but is closer to Asn127 (3.4 Å from Asn127 $N^{\delta 2}$; Fig. 2). No acetate, the product of the reaction of the catalase with peracetic acid, is observed in the distal side nor elsewhere, indicating that it flows out rapidly from the main channel.

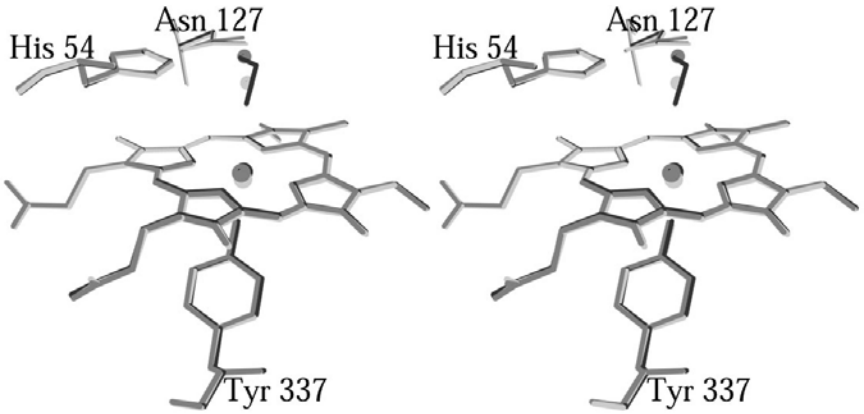

Figure 2
Close-up view of the active-site region of the native, compound I and formic acid complex structures of PMC. These three structures are coloured light grey, grey and black, respectively, and are drawn in stereo. Haem Fe atoms are represented as large balls. Water molecules and the O atom of the compound I oxoferryl group are displayed as small balls. The formic acid molecule is represented as black sticks.

The C^{α} traces of frozen native PMC and PMC compound I can be superimposed with an r.m.s. displacement of 0.3 Å. The maximum deviation between atom pairs is of 3.8 Å and occurs at residue Pro360 of the 359–362 loop. Residues of this loop are accessible to solvent and are usually poorly defined in the PMC electron-density maps. These residues are also poorly conserved among the different catalase sequences. Furthermore, variations between catalase structures are observed in the C^{α} traces at this region. Thus, there is no evidence to link the displacement of this loop with the formation of compound I.

On the other hand, changes are observed in the 'solute'-binding site when a glycerol is modelled at this location as in the native, although the positions of neighbouring amino-acid residues are unchanged. In contrast, modelling of a sulfate molecule at this position fits in the $2F_o - F_c$ and $F_o - F_c$ electron-density maps well. This substitution again shows the possibility of traffic inside the tetramer. The binding of an unidentified strong scatterer at this site had been already reported in the 2.7 Å time-resolved structure of PMC compound I (Gouet *et al.*, 1996). This solute-binding site might be characteristic of PMC, with a basic feature arising from the presence of non-conserved histidines and of an arginine. No heteroatoms have been observed at this location in the other structures of catalase (Bravo *et al.*, 1999; Mate *et al.*, 1999; Murshudov *et al.*, 1992; Fita & Rossmann, 1985) and the relationship between these solvent movements in PMC and the catalytic mechanism are not straightforward. However, a tyrosyl radical was observed at this position in bovine liver catalase when compound I was formed with an excess of peroxoacetic acid (Ivancich *et al.*, 1997; Andreoletti *et al.*, 2001). Thus, it seems that the formation of compound I can influence the distribution of electronic charges on amino-acid residues present in this region.

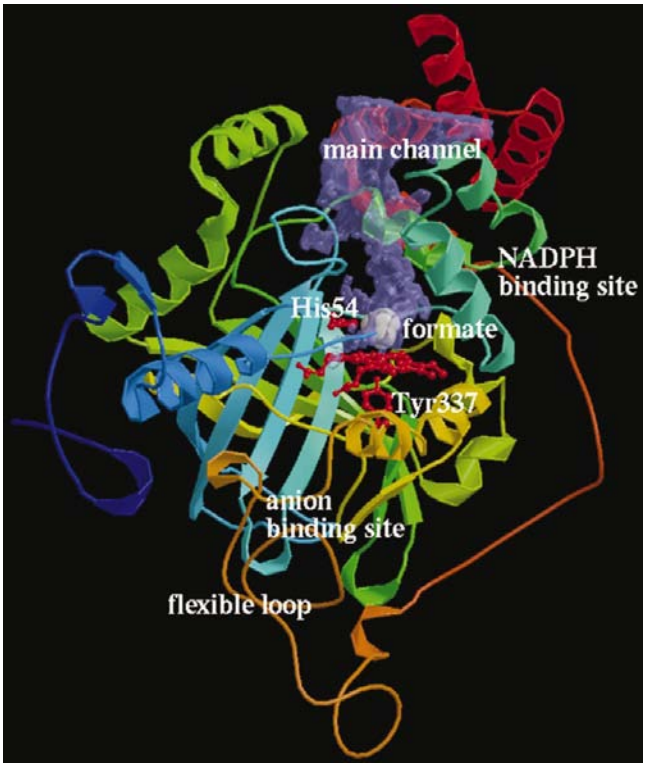

Figure 3
PMC monomer in complex with formic acid. The ribbon representation is colour-ramped from the N-terminus in blue to the C-terminus in red. The haem and the side chains of the two fundamental residues distal His54 and proximal Tyr337 are shown in red. Formic acid is represented in white in cpk mode. The main channel is rendered as a blue cloud.

Finally, movements of associated solvent molecules have been observed at the entrance of the main channel, as seen in the time-resolved structure of PMC compound I. They are likely to arise from the motion of peroxoacetic acid towards the active site.

3.4. Movement of water molecules within the active site of PMC during the catalytic cycle

The role of water molecules within the active site of catalases seems important to orient the enzymatic reaction towards the peroxidatic or the catalatic way (Jones, 2001). Jones (2001) proposed that a reversible equilibrium specific to catalases should take place between a 'wet' compound I, with a bound water molecule, and a 'dry' compound I without water. The enzymatic mechanism would be as follows:

$$\text{Compound I } (H_2O) \leftrightarrow \text{Compound I} + H_2O \quad (5)$$

$$\text{Compound I} + H_2O_2 \rightarrow \text{Catalase} + H_2O + O_2 \quad (6)$$

$$\text{Compound I } (H_2O) + H_2O_2 \rightarrow \text{Compound II} \quad (7)$$

The equilibrium (5) would be shifted to the right for catalase in order to promote the reaction with H_2O_2 (6). The reaction (7), a single-electron reduction of compound I typical of the peroxidatic way, would yield inactive catalase compound II (Chance, 1950; Nicholls *et al.*, 2001). If formic acid takes the place of a catalase substrate (such as peroxoacetic acid) used to form compound I, the water molecule present in the native structure (Fig. 1*a*) is displaced by the substrate (Fig. 1*b*). A water molecule reappears when compound I is formed, generating so-called 'wet' compound I (Fig. 1*c*). This implies that the water molecule should be released again to achieve the catalatic reaction, slowing down the traffic of H_2O_2 in the main channel.

In summary, the present structures show that the reaction of the catalase with substrate or inhibitor does not produce large-scale rearrangements of the protein. However, movements of solvent molecules are observed not only locally into the active site, but also far away at the entrance of the main channel leading to the haem distal side and in a distant cavity on the haem-proximal side.

This work was supported by the Commissariat à l'Energie Atomique (CEA) and the Centre National de la Recherche Scientifique (CNRS).

References

Aalten, D. M. F. van, Bywater, R., Findlay, J. B. C., Hendlich, M., Hooft, R. W. W. & Vriend, G. (1996). *J. Comput. Aided Mol. Des.* **10**, 255–262.

Andreoletti, P., Gambarelli, S., Sainz, G., Stojanoff, V., White, C., Desfonds, G., Gagnon, J., Gaillard, J. & Jouve, H. M. (2001). *Biochemistry*, **40**, 13734–13743.

Andreoletti, P., Sainz, G., Jaquinod, M., Gagnon, J. & Jouve, H. M. (2003). *Proteins*, **50**, 261–271.

Bravo, J., Fita, I., Gouet, P., Jouve, H. M., Melik-Adamyan, W. & Murshudov, G. N. (1997). *Oxidative Stress and the Molecular Biology of Antioxidant Defences*, edited by J. G. Scandalios, pp. 407–445. Cold Spring Harbor, USA: Cold Spring Harbor Laboratory Press.

Bravo, J., Mate, M. J., Schneider, T., Switala, J., Wilson, K., Loewen, P. C. & Fita, I. (1999). *Proteins*, **34**, 155–166.

Brünger, A. T., Adams, P. D., Clore, G. M., DeLano, W. L., Gros, P., Grosse-Kunstleve, R. W., Jiang, J.-S., Kuszewski, J., Nilges, M., Pannu, N. S., Read, R. J., Rice, L. M., Simonson, T. & Warren, G. L. (1998). *Acta Cryst.* D**54**, 905–921.

Chance, B. (1950). *Biochem. J.* **46**, 387–402.

Collaborative Computational Project, Number 4 (1994). *Acta Cryst.* D**50**, 760–763.

Dunford, H. B. (1999). *Heme Peroxidases.* New York: John Wiley & Sons.

Esnouf, R. M. (1997). *J. Mol. Graph.* **15**, 132–134.

Fita, I. & Rossmann, M. G. (1985). *J. Mol. Biol.* **185**, 21–37.

Gouet, P., Jouve, H. M. & Dideberg, O. (1995). *J. Mol. Biol.* **249**, 933–954.

Gouet, P., Jouve, H. M., Williams, P. A., Andersson, I., Andreoletti, P., Nussaume, L. & Hajdu, J. (1996). *Nature Struct. Biol.* **3**, 951–956.

Hershberg, R. D. & Chance, B. (1975). *Biochemistry*, **14**, 3885–3891.

Hewson, W. J. & Hager, L. P. (1979). *The Porphyrins*, edited by D. Dolphin, Vol. 7, pp. 295–332. New York: Academic Press.

Ivancich, A., Jouve, H. M., Sartor, B. & Gaillard, J. (1997). *Biochemistry*, **36**, 9356–9364.

Jones, P. (2001). *J. Biol. Chem.* **276**, 13791–13796.

Jouve, H. M., Andreoletti, P., Gouet, P., Hajdu, J. & Gagnon, J. (1997). *Biochimie*, **79**, 667–671.

Jouve, H. M., Beaumont, F., Léger, I., Foray, J. & Pelmont J. (1989). *Biochem. Cell Biol.* **67**, 271–277.

Jouve, H. M., Gaillard, J. & Pelmont, J. (1984). *Can. J. Biochem. Cell Biol.* **62**, 935–944.

Jouve, H. M., Gouet, P., Boudjada, N., Buisson, G., Kahn, R. & Duee, E. (1991). *J. Mol. Biol.* **221**, 1075–1077.

Maj, M., Loewen, P. & Nicholls, P. (1998). *Biochim. Biophys. Acta*, **1384**, 209–222.

Mate, M. J., Zamocky, M., Nykyri, L. M., Herzog, C., Alzari, P. M., Betzel, C., Koller, F. & Fita, I. (1999). *J. Mol. Biol.* **286**, 135–149.

Melik-Adamyan, W., Bravo, J., Carpena, X., Switala, J., Mate, M. J., Fita, I. & Loewen, P. C. (2001). *Proteins*, **44**, 270–281.

Millar, F., Wrigglesworth, J. M. & Nicholls, P. (1981). *Eur. J. Biochem.* **117**, 13–17.

Murshudov, G. N., Melik-Adamyan, W. R., Grebenko, A. I., Barynin, V. V., Vagin, A. A., Vainshtein, B. K., Dauter, Z. & Wilson, K. S. (1992). *FEBS Lett.* **312**, 127–131.

Nicholls, P. (1961). *Biochem. J.* **81**, 365–374.

Nicholls, P., Fita, I. & Loewen, P. C. (2001). *Adv. Inorg. Biochem.* **51**, 51–106.

Nicholls, P. & Schonbaum, G. R. (1963). *The Enzymes*, edited by P. D. Boyer, H. Lardy & K. Myrback, Vol. 8, pp. 147–225. New York: Academic Press.

Otwinowski, Z. & Minor, W. (1997). *Methods Enzymol.* **276**, 307–326.

Poulos, T. L. (2000). *The Porphyrin Handbook*, edited by K. M. Kadish, K. M. Smith & R. Guilard, Vol. 4, pp. 189–218. New York: Academic Press.

Putnam, C. D., Arvai, A. S., Bourne, Y. & Tainer, J. A. (2000). *J. Mol. Biol.* **296**, 295–309.

Roussel, A. & Cambillau, C. (1989). *Silicon Graphics Geometry Partners Directory*, pp. 77–79. Mountain View, CA, USA: Silicon Graphics.

Schonbaum, G. R. & Chance, B. (1976). *The Enzymes*, edited by P. D. Boyer, Vol. 13, pp. 363–408. New York: Academic Press.

Switala, J. & Loewen, P. C. (2002). *Arch. Biochem. Biophys.* **401**, 145–154.

Vuk-Pavlovic, S. & Williams-Smith, D. L. (1977). *Biochemistry*, **16**, 5465–5470.

Williams-Smith, D. L. & Morrison, P. J. (1975). *Biochim. Biophys. Acta*, **405**, 253–261.

Acta Crystallographica Section D
Biological Crystallography
ISSN 0907-4449

addenda and errata

Structural studies of *Proteus mirabilis* catalase in its ground state, oxidized state and in complex with formic acid. Erratum

Pierre Andreoletti,[a] Anaïs Pernoud,[b] Germaine Sainz,[c] Patrice Gouet[b] and Hélène Marie Jouve[d]*

[a]Avidis S.A., Biopôle Clermont-Limagne, 63360 Saint-Beauzire, France, [b]IBCP–Laboratoire de Bio-Cristallographie, 7 Passage du Vercors, 69367 Lyon CEDEX 07, France, [c]European Synchrotron Radiation Facility, 6 Rue Jules Horowitz, BP 220, F-38043 Grenoble CEDEX, France, and [d]Institut de Biologie Structurale Jean-Pierre Ebel, CEA/CNRS/UJF, 41 Rue Jules Horowitz, 38027 Grenoble CEDEX 1, France. Correspondence e-mail: jouve@ibs.fr

In the paper by Andreoletti *et al.* [(2003), *Acta Cryst.* D**59**, 2163–2168] an incorrect version of Figure 2 was published. The correct version is given below.

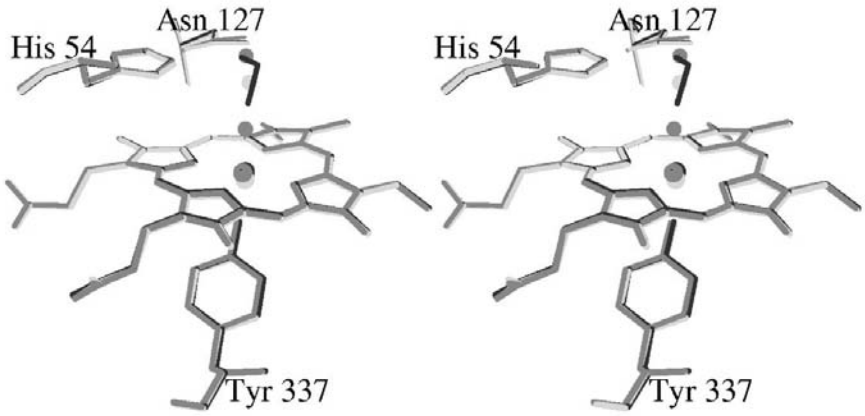

Figure 2
Close-up view of the active-site region of the native, compound I and formic acid complex structures of PMC. These three structures are coloured light grey, grey and black, respectively, and are drawn in stereo. Haem Fe atoms are represented as large balls. Water molecules and the O atom of the compound I oxoferryl group are displayed as small balls. The formic acid molecule is represented as black sticks.

References

Andreoletti, P., Pernoud, A., Sainz, G., Gouet, P., Jouve, H. M. (2003). *Acta Cryst.* D**59**, 2163–2168.

 DOI: 10.1107/S0907444904001271